SSRG International Journal of Civil Engineering
ISSN: 2348-8352/ https://doi.org/10.14445/23488352/IJCE-V11I7P101

Volume 11 Issue 7, 1-19, July 2024

Original Article

Parametric Analysis Studies of the Vibrations of a Multi-Cable-Stayed Beam Resting on Elastic Supports

Mohamed Berjal[1], Ahmed Adri[2], Omar Outassafte[3], Issam El Hantati[4], Yassine El Khouddar[5], Mohamed Rjilatte[6], Rhali Benamar[7]

[1,2,3,5,6]*Laboratory of Mechanics Production and Industrial Engineering (LMPGI), High School of Technology (ESTC), Hassan II University of Casablanca, Morocco.*
[4]*Laboratory for Control and Mechanical Characterization of Materials and Structures (LCCMMS), ENSEM, Hassan II University of Casablanca, Morocco.*
[5]*Engineering of Complex Systems and Structures (ECSS), ENSAM, Moulay Ismail, Meknes, Morocco.*
[7]*Mohammed V University of Rabat, EMI-Rabat, LERSIM, Rabat, Morocco.*

[1]*Corresponding Author : mohamed.berjal.doc22@ensem.ac.ma*

Received: 03 May 2024 Revised: 03 June 2024 Accepted: 02 July 2024 Published: 31 July 2024

Abstract *- Cable-stayed beams represent one of the most widely discussed topics in the current scientific world, attracting immense attention from researchers in the fields of civil and mechanical engineering. To investigate the behavior of transverse vibrations in the plane of coupled cables and beams resting on elastic supports, a linear single-beam and multi-cable mechanical model was developed. In this work, general expressions are derived for the multi-cable beam based on the fundamental principle of the Euler-Bernoulli method. By taking into account the impact of nonlinear geometric factors caused by the initial sag of the cables, the multi-cable beam model by segments is analyzed. Firstly, using the example of a double-cabled beam as a case study for the clamped-clamped, clamped-simply supported, and simply supported at both ends beam configurations, the solution of the free vibration eigenvalues in the plane is performed by combining the boundary and continuity conditions using the robust Newton-Raphson algorithm. The results obtained are compared with those of the reference articles and show good agreement. Next, the analysis is extended to a two-cable supported beam resting on elastic supports. A parametric study is conducted to evaluate the effectiveness of these supports in mitigating the structural vibrations of the cable-stayed beam. Different configurations are explored, including the variation of the stiffness, position, and number of elastic supports, ranging from a single elastic support to two and three elastic supports. The impact of these elastic supports on the dynamic behavior of the beam is examined in detail, thus promoting the improvement of the dynamic performance and flexibility of cable-stayed structures. This study demonstrates that strategic manipulation of the stiffness and configuration of elastic supports is essential for improving the dynamic performance and robustness of cable-stayed structures. This not only ensures the safety and reliability of the structure but also optimizes its performance under different loading scenarios, making this approach an effective solution for advanced applications in civil and mechanical engineering.*

Keywords *- Cable-stayed beam vibration, Elastic support, Frequency analysis, Modal analysis, Linear vibration, Mode shape, Newton-Raphson algorithm, Parametric analysis.*

1. Introduction

Cable-beam coupled structures, composed of flexible cables and elastic beams, offer significant structural advantages in the fields of civil and mechanical engineering. These structural advantages are manifested in the realization of long-span structures, ease of construction, affordable construction costs, the realization of optimized structures, and better structural performance under the effect of loads (permanent, operating, or thermal) and constraints. This allows for wide adaptation and application in large-scale real projects (buildings, bridges, footbridges, etc.).

Over the past few decades, the need for large-span projects has continued to increase day by day. Long spans pose new challenges in terms of calculation (maximum deflection, displacement, deformation, and stresses) and construction (construction technologies and investment in execution means). With this requirement for long spans, the dynamic behavior of structures becomes increasingly complex and sensitive to small perturbations due to coupling interactions, leading to and requiring carefully controlled structural analysis. It is, therefore, essential to analyze and study the overall dynamic behavior and coupling properties of cables and beams from different perspectives.

Suspended cables in reinforced, pre-stressed, and steel concrete bridges, fixed and mobile cranes and pylons, as well as beams and cables in lattice structures, can all be considered cable-beam coupled and composite structures.

Up to now, numerous scientific studies have been conducted on beam-cable models subjected to various types of loads and disturbances, with the aim of exploring the interaction mechanisms. In 2020, Y. Cong H. Kang [1] first proposed an in-depth study of the dynamic behavior of cable-stayed bridges, using a linear multi-cable beam model to analyze vibrations in the horizontal and vertical planes. Subsequently, the co-authors [2] discussed the modeling of a cable-stayed bridge with CFRP cables, performing a modal analysis of the system. The examination focused on the impact of increasing the axial stiffness of the cables and the flexural stiffness of the beams on the system's vibration frequencies. T. Guo [3] explores the dynamic interactions between the cables and the bridge girder in cable-stayed structures by developing an asymptotically reduced coupled model. X. Su [4] studies free vibrations in the plane of a multi-cable stayed bridge using the transfer matrix method. Y. Cong [5] and H. Kang [6] deal with the analysis of the dynamics of cable-stayed bridges, considering both the nonlinear geometry of the cables and shallow arches using methods such as the Finite Element Method (FEM) solution and the application of the Galerkin method.

Cao et al. [7] investigated the vibrations of a complex cable-stayed bridge with four cables and girders. They derived both linear and nonlinear differential vibration equations, both in-plane and out-of-plane. The research conducted by Kang et al. [8] involved applying the theory of vibrations of taut cables and Euler beams to develop a theory of in-plane internal vibrations. R. Ma [9] examines the static response and dynamic modal properties of a 1088m main span cable-stayed bridge under strong winds, focusing on the effect of cable vibration on the overall bridge behavior. C. Gentile et F. M. Y. Cabrera [10] analyze the dynamic behavior of two recently constructed curved cable-stayed bridges using large-scale tests and theoretical models. X. Su and H. Kang [11] examine a novel nonlinear system, a cable-stayed beam model with a tuned mass damper. The coauthors of [12] have developed a novel dynamic theory and analysis of the nonlinear dynamic behavior of a cable-stayed bridge model under harmonic excitation, showing that partial differential equations solved via Galerkin's method reveal complex phenomena such as asymmetric jumps in the cables during subharmonic resonance. The same coauthors have studied the energy transfer between the deck and cables in cable-stayed bridges through resonance analysis, taking into account the coupling effect of adjacent cables.

Considering a bridge model in its entirety, the mode shapes of the cable-stayed beam were determined by Wang et al. [13] using a piecewise function. Zhu et al. [14] developed a continuous model for an inclined cable and a nonlinear cable-stayed beam, incorporating an in-plane degree of freedom to account for cable damage. The studies [15] and [16] focus on the modeling and analysis of the dynamic behavior of cable-stayed beam structures. They use methods such as Galerkin discretization and the scale method. V. Gattulli et al. [17] and M. Lepidi [18] propose analytical models to study the nonlinear interactions between beam and cable dynamics in cable-stayed systems.

However, work on beams resting on elastic supports has been addressed repeatedly. P. Chang [19] proposed an exact and explicit solution for the free vibrations of Euler-Bernoulli beams supported by an arbitrary number of translational supports at arbitrary positions under variable boundary conditions. A. Ahmed previously established the theoretical formulation of the problem of nonlinear transverse vibrations of Bernoulli-Euler beams resting on elastic supports and masses. I. El Hantati already studied the nonlinear vibrations of beams with elastic supports (translation and rotation) at the end using Euler-Bernoulli and von Karman's theories to calculate their modes and frequencies. O. Outassafte explored the geometric nonlinearity in the vibrations of a shallow arch elastically restrained at the ends by elastic support (translation and rotation).

Linear and nonlinear vibrations using Euler-Bernoulli beam theory have been studied multiple times. For instance, El Hantati before examined the nonlinear free and forced vibrations of tapered beams based on Euler-Bernoulli beam theory and von Karman's geometric nonlinearity assumptions, determining the nonlinear frequencies and modes as well as the associated stress distributions. Outassafte O. earlier investigated the geometrical nonlinearity in the in-plane free vibration of an inextensible circular arch with uniform cross-section and elastic rotational restraints at both ends. El Khouddar Y. was studied the nonlinear free and forced vibrations subjected to harmonic excitations of laminated composite beams using Euler-Bernoulli beam theory and Green-Lagrange's geometric nonlinearity hypothesis. In earlier, Adri A. analytically analyzed the frequencies and mode shapes of a clamped beam carrying a point mass at different positions, conducting a parametric study using the Newton-Raphson method to solve the transcendental frequency equation.

Indeed, the analysis of cable-stayed beams under thermal loads has been carried out in some case studies. Y. Zhao [20] studied the effect of temperature on the vibration of a cable-stayed beam. The thermal effect is considered by using two non-dimensional factors for the cable tension force and sag. In addition to research efforts to understand the response of structures to thermal loads, a study was also conducted by Y. El Khouddar previously studied of free and forced vibrations of a beam made of functionally graded materials while taking into account temperature variations. The nonlinear

equilibrium equations are obtained by Hamilton's principle and solved by a multimode approach. A parametric study explores the influence of various factors, including temperature variations, on nonlinear vibration solutions. The analysis of bridges by structural monitoring systems in [21] allows for real-time monitoring of the condition of bridges. By eliminating the effects of dynamic loads, the data can represent the response of the structure to dead and thermal loads only, offering a promising tool for identifying damage.

To date, previous research has not fully addressed the complexity of systems where beams and cables are coupled and rest on translational elastic supports while being subjected to variations in position, stiffness, and number of elastic supports. This gap in research is particularly significant as it could provide essential insights into global structural behavior, which is vital for the development of active monitoring systems tailored to such structures.

With this motivation, the present study focuses on examining a cable-stayed beam supported by elastic supports. Firstly, the study begins with the analysis of free vibrations of a double-cabled beam with different clamped-clamped, clamped-simply supported, and simply supported beam configurations using an eigenvalue problem approach. The Newton-Raphson algorithm is implemented to handle boundary and continuity conditions.

Next, the study moves on to a cable-stayed bridge with two cables and elastic supports. A series of parametric analyses is conducted to evaluate the impact of these supports on vibration reduction. Various stiffness, positioning, and number of support configurations are explored, demonstrating the value of elastic supports in enhancing the dynamic performance and robustness of cable-stayed structures.

The objective of this study is to address the identified gaps in the current literature by providing an in-depth analysis of the dynamic behavior of cable-stayed beams, with particular attention to the effects of elastic supports. The results obtained can serve as a foundation for the future development of monitoring and structural optimization systems, thus contributing to the design of safer and more efficient structures.

2. Elastic Support

Bridge bearings play a pivotal role in the dynamic behavior of bridges, particularly in the realm of mechanical vibrations. These devices, often regarded as elastic supports, enable structures to bear vertical loads while allowing horizontal movements and rotations necessary to accommodate deformations and thermal expansions. Elastic supports can be composed of various materials and mechanisms, such as neoprene pads, pot bearings, or disc bearings, which offer varying degrees of stiffness and flexibility. By optimizing support rigidity, it is possible to reduce internal stresses and enhance the durability and stability of the structure.

These devices balance the necessary rigidity to support vertical loads and the flexibility to allow for anticipated deformations, utilizing combinations of steel plates and rubber. Including the rigidity of the bearings in structural calculation models is essential for precise analysis, especially in contexts where these supports can help reduce forces.

Accurate analysis and modeling of elastic supports are crucial for predicting the vibrational behavior of bridges under diverse loading conditions. This enables the design of safer and more resilient infrastructure. Parametric studies of the vibrations of a multi-cable-stayed beam resting on elastic supports offer valuable insights into understanding the influence of support properties on the natural frequencies and vibration modes of the structure.

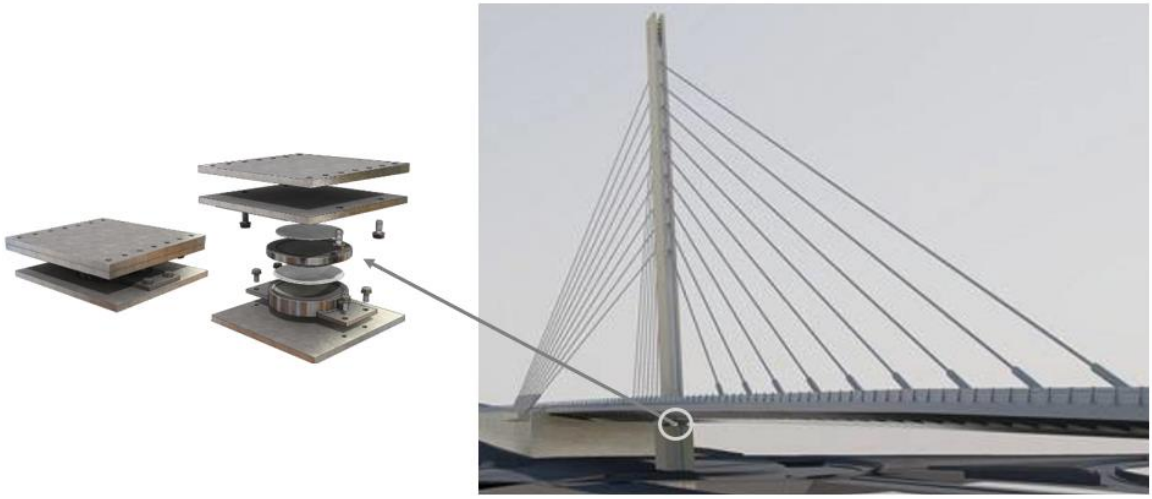

Fig. 1 Illustration of an elastomeric bearing (elastic support) in a cable-stayed brid

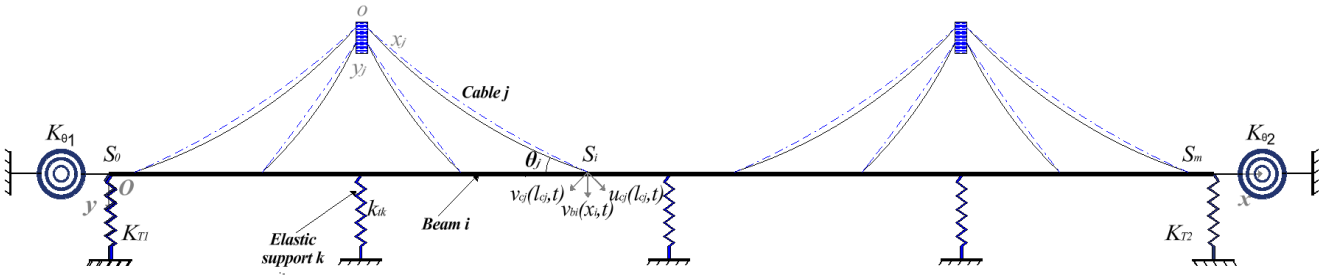

Fig. 2 Configurations of multiple cable-stayed beams with multiple elastic supports under thermal loads

3. Problem Formulation

3.1. Basic Configuration and Hypotheses

In this article, we present a simplified model of a cable-stayed bridge deck using a beam with multiple cables (as illustrated in Figure 2). This model focuses on analyzing in-plane movements within the deck. The beam ends are simply supported, and each cable is anchored to the rigid tower at its upper end and connected to the beam at its other end, designated as junctions s_j. The different beam support scenarios that will be considered in the first section of the work include Clamped-Clamped (CC), Clamped-Simply supported (CS), and Simply Supported (SS) at both end configurations. These cables are inclined at an angle θ relative to the horizontal plane. To account for the flexibility of the bridge supports, the beam is modeled with translational elastic supports of stiffness $K_{ti}(i = 1, 2, \dots, n)$ at mid-span and both ends. The junctions effectively divide the beam into individual segments, each modeled as a separate beam element i. The entire structure is subjected to a uniform thermal load due to a temperature change $\Delta T = T - T_0$, where ΔT represents the difference between the current temperature T and a reference temperature T_0. While real bridges experience thermal gradients across the depth of the beam, such complexities are not considered in this simplified model for better tractability.

The cable displacement components precisely describe the static equilibrium configuration of this model of beam u_{cj}, v_{cj}, w_{cj} $(j = 1, 2, \dots, n)$, and by the transverse displacements of the beam v_{bi} $(i = 1, 2, \dots, n)$, thereby emphasizing the importance of the elements in understanding the system, as illustrated in Figure 2.

It is assumed that the deformation of each cable follows a parabolic trajectory $y_{cj} = 4d_{cj}[x_{cj}/l_{cj} - (x_{cj}/l_{cj})^2]$, where the deflection ratio d_{cj} relative to the cable length l_{cj} is less than $1/10$.

The towers in which the cables are anchored are considered rigid due to minimal vibrations affecting them, which has been confirmed by experimental tests and finite element analysis [11]. Given the high stiffness ratio (axial to flexural) during transverse vibrations, the axial displacement of the beam is negligible, as demonstrated by $E_b A_b/l_b >> 48E_b A_b/l_b^3$. Considering the minimal impact of the horizontal component of cable tension on the overall behavior of the system [22], this component can be disregarded. Furthermore, the hypotheses presented in [22] are retained for this analysis.

- Material Hypothesis and Linear Behavior: The cables and the beam are assumed to behave linearly and elastically, with a proportional relationship between stress and deformation.
- Description of Axial Deformations of Cables: Lagrangian deformation of the median line is used to describe the elongation of the cables.
- Simplifications Concerning the Cables: Longitudinal inertia forces, stiffnesses related to flexure, torsion, and shear of the cables are neglected.
- Simplifications Concerning the Beam: For the beam, axial deformations, torsional and shear deformations, as well as geometric nonlinearities, are neglected.

3.2. Equations of Motion and Boundary Conditions

3.2.1. Beams Suspended by Two Cables

In accordance with the assumptions mentioned above, Hamilton's principle is employed to derive the equations of motion for the composite system in the plane, following appropriate reduction.

$$m_{bi}\frac{\partial^2 v_{bi}^*(x_i)}{\partial t^2} + \xi_{bi}^*\frac{\partial v_{bi}(x_i)}{\partial t} + E_{bi}I_{bi}v_{bi}^{iv*}(x_i) = 0 \text{ where } s_{i-1} < x_i < s_i$$

$$m_{cj}\frac{\partial^2 v_{cj}^*}{\partial t^2} + \xi_{cj}^*\frac{\partial v^*{}_{cj}}{\partial t} - [H_{cj}\frac{\partial^2 v_{cj}^*}{\partial x_{cj}^2} + E_{cj}A_{cj}(\frac{\partial^2 y_j^*}{\partial x_{cj}^2} + \frac{\partial^2 v_{cj}^*}{\partial x_{cj}^2})e_j^*(t)] = 0 \quad (1)$$

e_{cj} represents the uniform dynamic elongation of cable j :

$$e_j{}^*(t) = \frac{u_{cj}^*(l_{cj}, t)}{l_{cj}} + \frac{1}{l_{cj}}\int_0^{l_{cj}}\left(\frac{\partial y_j^*}{\partial x_j}\frac{\partial v_{cj}^*}{\partial x_j} + \frac{1}{2}\left(\frac{\partial v_{cj}^*}{\partial x_j}\right)^2\right)dx_j^* \quad (2)$$
$$(j = 1, 2, \dots, n;\ i = 1, 2, \dots, n+1)$$

The terms $\frac{\partial^2 v_{cj}^*}{\partial t^2}$ and $\frac{\partial^2 v_{bi}^*(x_i)}{\partial t^2}$ represent the second derivatives with respect to time, while $v_{bi}^{iv^*}$ is the fourth derivative with respect to the coordinates; $\frac{\partial y_j^*}{\partial x_j}$, $\frac{\partial^2 y_j^*}{\partial x_{cj}{}^2}$, $\frac{\partial v_{cj}^*}{\partial x_j}$ and $\frac{\partial^2 v_{cj}^*}{\partial x_{cj}{}^2}$ respectively represent the first and second derivatives with respect to coordinates. $m_{cj}, \xi_{cj}^*, m_{bi}$ and ξ_{bi}^* denote the unit mass and the damping coefficient of the cable j and segment i. H_{cj} is the horizontal component of the initial tension of diagonal cable j in the local coordinate system. E_{cj}, A_{cj} are the Young's modulus and the cross-sectional area of cable j. E_{bi} *and* I_{bi} represent Young's modulus and the second moment of inertia in the plane for beam segment i. ${e_j}^*(t)$ denotes the uniform dynamic elongation of cable j.

The analysis is based on the assumption regarding the beam's end conditions, as discussed above. The upper end of the cable is assumed to be fixed to the bridge tower, while the lower end is connected to the beam. Consequently, the composite system must adhere to the continuity conditions and the boundary conditions presented above.

$$
\begin{gathered}
v_{b1}^*(x_j,t)\big|_{x_j=0,t} = v_{b(n+1)}^*(x_j,t)\big|_{x_j=l_b,t}, \\
\left.\frac{\partial^2 v_{b1}^*}{\partial {x_j}^2}\right|_{x_j=0,t} = 0, v_{cj}^*(x_j,t)\big|_{x_j=0,t} = 0, \\
\left.\frac{\partial^2 v_{bj}^*}{\partial {x_j}^2}\right|_{x_j=s_j^*,t} = \left.\frac{\partial^2 v_{b(j+1)}^*}{\partial {x_j}^2}\right|_{x_j=s_j^*,t}, \\
\left.\frac{\partial v_{bj}^*}{\partial x_j}\right|_{x_j=s_j^*,t} = \left.\frac{\partial v_{b(j+1)}^*}{\partial x_j}\right|_{x_j=s_j^*,t}, \\
\left.\frac{\partial^{2 v_{b(n+1)}^*}}{\partial {x_j}^2}\right|_{x_j=l_b,t} = 0, \\
v_{bj}^*(x_j,t)\big|_{x_j=s_j^*,t} = v_{b(j+1)}^*(x_j,t)\big|_{x_j=s_j^*,t}, \\
u_{cj}^*(x_j,t)\sin\theta + v_{cj}^*(x_j,t)\cos\theta\big|_{x_j=l_{cj},t} \\
= v_{bj}^*(x_j,t)\,\big|_{x_j=s_j^*,t}, \\
\left(u_{cj}^*(x_j,t)\cos\theta - v_{cj}^*(x_j,t)\sin\theta\right)\big|_{x_j=l_{cj},t} = 0, \\
u_{cj}^*(x_j,t)\big|_{x_j=l_{cj},t} = v_{bj}^*(x_j,t)\sin\theta_j\big|_{x_j=s_j^*,t}, \\
v_{cj}^*(x_j,t)\big|_{x_j=l_{cj},t} = v_{bj}^*(x_j,t)\cos\theta_j\big|_{x_j=s_j^*,t}, \\
(j=1,2,\dots,n)
\end{gathered}
\tag{3}
$$

The application of Hamilton's principle of variation [7] also allows for the derivation of the following mechanical boundary conditions:

$$
\begin{aligned}
& E_{bj}I_{bj}\frac{\partial^3 v_{bj}^*(s_j^*,t)}{\partial {x_j^*}^3} \\
& - E_{b(j+1)}I_{b(j+1)}\frac{\partial^3 v_{b(j+1)}^*(s_j^*,t)}{\partial {x_j^*}^3} \\
& = E_{cj}A_{cj}e_{cj}^*(t)\sin\theta_j + [H_{cj}\frac{\partial v_{cj}^*(l_{cj},t)}{\partial t} \\
& + E_{cj}A_{cj}e_{cj}^*(t)(\frac{\partial v_{cj}^*(l_{cj},t)}{\partial x_{cj}} \\
& + \frac{\partial y_{cj}^*(l_{cj})}{\partial x_{cj}})]\cos\theta_j \\
& (j=1,2,\dots,n)
\end{aligned}
\tag{4}
$$

To reach more general conclusions, the following dimensionless variables are introduced:

$$
\begin{gathered}
x^j = \frac{x_j^*}{l_{cj}}, \tau = \omega_0 t, y^i\frac{y_j^*}{l_{cj}}, u^j = \frac{u_j^*}{l_{cj}}, v^j = \frac{v_j^*}{l_{cj}}, \\
\gamma_j = \frac{l_b}{l_{cj}}, s^j = \frac{s^*}{l_b}, \xi_{cj} = \frac{\xi_{cj}^*}{m_{cj}\omega_0}, d_j = \frac{d_j^*}{l_{cj}}, \\
\mu = \frac{E_c A_c}{H_c}, {\beta_b}^4 = \frac{m_b {l_b}^4 {\omega_0}^2}{E_b I_b}, \xi_{bi} = \frac{{\xi_{bi}}^*}{m_{bi}\omega_0}, \\
{\beta_c}^2 = \frac{m_c {l_c}^2 {\omega_0}^2}{H_c}, \chi = \frac{E_b I_b}{{l_b}^2 E_c A_c}, \mu^j = \frac{E_{cj}A_{cj}}{H_{cj}}, \\
(j=1,2,\dots,n; i=1,2,\dots,n+1)
\end{gathered}
\tag{5}
$$

The introduction of dimensionless variables allows for the reformulation of Equations (1) to (4) in a dimensionless form. By recasting the equations in dimensionless terms, more general and unit-independent equations are obtained, which facilitates the interpretation of results and comparison with other studies in the field.

$$
\begin{aligned}
& {\beta_{bi}}^4\left(\frac{\partial^2 v_{bi}}{\partial t^2} + \xi_{bi}\frac{\partial v_{bi}}{\partial t}\right) + \frac{\partial^4 v_{bi}}{\partial x_i^4} = 0 \\
& {\beta_{cj}}^2\left(\frac{\partial^2 v_{cj}}{\partial t^2} + \xi_{bj}\frac{\partial v_{bj}}{\partial t}\right) - \frac{\partial^4 v_{cj}}{\partial x_{cj}^4} - \mu e \\
& \left(\frac{\partial^3 y_{cj}}{\partial x_{cj}^3} + \frac{\partial^3 v_{cj}}{\partial x_{cj}^3}\right) = 0 \\
& (j=1,2,\dots,n; i=1,2,\dots,n+1)
\end{aligned}
\tag{6}
$$

The expression for the uniform dynamic elongation of the cable can be derived using the boundary conditions of Equation (3) as follows:

$$
e_j = v_{cj}(1,t)\tan\theta_j \tag{7}
$$

$$+\int_0^1\left(\frac{\partial y_{cj}}{\partial x_j}\frac{\partial v_{cj}}{\partial x_j}+\frac{1}{2}\left(\frac{\partial v_{cj}}{\partial x_j}\right)^2\right)dx_j$$
$$(j=1,2,\dots,n)$$

In the context of this analysis, the boundary conditions are formulated in dimensionless terms as follows:

$$\begin{gathered}v_{b1}(0,t)=v_{bm}(1,t)=0,\\ \left.\frac{\partial^2 v_{b1}}{\partial {x_j}^2}\right|_{x_j=0,t}=0,\ \left.\frac{\partial^2 v_{bm}}{\partial {x_j}^2}\right|_{x_j=1,t}=0,\\ \left.\frac{\partial v_{bj}}{\partial x_j}\right|_{x_j=s_j,t}=\left.\frac{\partial v_{b(j+1)}}{\partial x_j}\right|_{x_j=s_j,t},\\ v_{bj}(s_j,t)=v_{b(j+1)}(s_j,t),v_{cj}(0,t)=0,\\ \left.\frac{\partial^2 v_{bj}}{\partial x_j^2}\right|_{x_j=s_j,t}=\left.\frac{\partial^2 v_{b(j+1)}}{\partial x_j^2}\right|_{x_j=s_j,t},\\ u_{cj}(1,t)\sin\theta_j+v_{c1}(1,t)\cos\theta_j=v_{bj}(s_j,t),\\ v_{cj}(1,t)=v_{bj}(s_j,t)\cos\theta_j,\\ E_{bj}I_{bj}\frac{\partial^3 v_{bj}(s_j,t)}{\partial x_j^3}-E_{b(j+1)}I_{b(j+1)}\frac{\partial^3 v_{b(j+1)}(s_j,t)}{\partial x_j^3}\\ =\\ E_{cj}A_{cj}e_{cj}(t)\sin\theta_j+\left(H_{cj}\frac{\partial v_{cj}(1,t)}{\partial t}+\right.\\ \left.E_{cj}A_{cj}e_{cj}(t)\left(\frac{\partial v_{cj}(1,t)}{\partial x_j}+\frac{\partial y_{cj}(1,t)}{\partial x_j}\right)\right)\cos\theta_j\end{gathered}\tag{8}$$

By simplifying the differential equation of the cable's motion and neglecting the higher-order terms and the nonlinear squared terms in the integral of the uniform dynamic elongation of the cable $e_{cj}(t)$, the equations for the undamped free vibrations of the cable and the beam are obtained as follows [23] :

$$\begin{gathered}{\beta_{cj}}^2\frac{\partial^2 v_{ci}}{\partial t^2}-\frac{\partial^2 v_{ci}}{\partial x_{cj}^2}-\mu\hat{e}_j\frac{\partial^2 y_{ci}}{\partial x_{cj}^2}=0\\ {\beta_{bi}}^4\frac{\partial^2 v_{bi}}{\partial t^2}+\frac{\partial^2 v_{bi}}{\partial x_i^4}=0\\ (j=1,2,\dots,n;i=1,2,\dots,m)\end{gathered}\tag{9}$$

In the equation above:

$$\hat{e}_j=v_{cj}(1,t)\tan\theta_j+\int_0^1\left(\frac{\partial y_{cj}}{\partial x_{cj}}\frac{\partial v_{cj}}{\partial x_{cj}}\right)dx_j\qquad(j=1,2,\dots,n)\tag{10}$$

By adopting a similar approach, the mechanical boundary conditions can be represented in a linear form, as illustrated below:

$$\begin{gathered}\frac{E_{bj}I_{bj}}{{l_b}^2}\frac{\partial^3 v_{bj}}{\partial x_j^3}(s_j,t)\\ -\frac{E_{b(j+1)}I_{b(j+1)}}{{l_b}^2}\frac{\partial^3 v_{b(j+1)}}{\partial x_j^3}(s_j,t)\\ =E_{cj}A_{cj}\hat{e}_{cj}(t)\sin\theta_j\\ +\left[H_{cj}\frac{\partial v_{cj}}{\partial t}(1,t)\right.\\ \left.+E_{cj}A_{cj}\hat{e}_{cj}(t)\frac{\partial y_{cj}}{\partial x_{cj}}(1,t)\right]\cos\theta_j\end{gathered}\tag{11}$$

Previous research has revealed the susceptibility of asymmetric bridges to damage induced by vibrations. Indeed, the concentration of vibratory energy on a limited number of cables can occur under certain circumstances when the excitation frequencies are close to the natural frequencies of localized modal shapes.

As a result, this work utilizes a model of a symmetric double-cable beam. Based on the theoretical principles previously discussed and considering a symmetrical configuration of cables anchored at one-third of the beam length with an angle of 30 degrees, the following variable substitutions will be made:

$$\begin{gathered}H_{cj}=H_c,d_j=d,\theta_j=\theta,m_{cj}=m_c,\gamma_{cj}=\gamma_c,\\ E_{cj}A_{cj}=E_cA_c,l_{cj}=l_c,m_{bi}=m_b,\\ E_{bi}I_{bi}=E_bI_b,\\ (j=1,2;\ i=1,2,3)\end{gathered}\tag{12}$$

Within this equation, d_j denotes the dimensionless deflection of the j-th cable. By employing the method of separation of variables, we formulate the following relationship:

$$\begin{gathered}v_{cj}=w_{cj}(x)e^{i(\omega/\omega 0)\tau};(j=1,2)\\ v_{bi}=w_{bi}(x)e^{i(\omega/\omega 0)\tau};(i=1,2,3)\end{gathered}\tag{13}$$

Additionally, the following equality can be established:$x_c=s=x$

After substituting Equation (13) into the linear vibration equations of the cable and beam, we obtain [24]:

$$\begin{gathered}{\beta_{cj}}^2w_{cj}+\frac{\partial^2 w_{cj}}{\partial x_{cj}^2}=8\mu d\hat{e}_j\ (j=1,2)\\ -{\beta_{bi}}^4w_{bi}+\frac{\partial^4 w_{bi}}{\partial x_i^4}=0\ (i=1,2,3)\end{gathered}\tag{14}$$

In which:

$$\hat{e}_j = w_{cj}(1)\tan\theta_j + \int_0^1 \left(\frac{\partial y_{cj}}{\partial x_{cj}}\frac{\partial w_{cj}}{\partial x_{cj}}\right) dx_{cj} \quad (j = 1,2) \tag{15}$$

The incorporation of linear and rotational elastic supports at both ends of the beam allows for the analysis of different structural configurations by varying the values of the rotational and translational stiffness constants, K_{T1}, K_{T2}, $K_{\theta 1}$ and $K_{\theta 2}$. These configurations include the fixed-fixed, fixed-simply supported, and simply supported at both ends cases. The boundary conditions for a beam segment supported by linear and rotational elastic supports on each side are detailed in the previous study.

$$\begin{aligned}
\left.\frac{\partial^3 w_{b1}}{\partial {x_i}^3}\right|_{x_i=0} &= -K_{T1}\, w_{b1}|_{x_i=0} \\
\left.\frac{\partial^2 w_{b1}}{\partial {x_i}^2}\right|_{x_i=0} &= K_{\theta 1}\left.\frac{\partial w_{b1}}{\partial x_i}\right|_{x_i=0} \\
\left.\frac{\partial^3 w_{b3}}{\partial {x_i}^3}\right|_{x_i=1} &= K_{T2}\, w_{b3}|_{x_i=1} \\
\left.\frac{\partial^2 w_{b3}}{\partial {x_i}^2}\right|_{x_i=1} &= -K_{\theta 2}\left.\frac{\partial w_{b3}}{\partial x_i}\right|_{x_i=1}
\end{aligned} \tag{16}$$

Furthermore, the associated boundary conditions are derived:

$$\begin{aligned}
w_{c1}(0) &= w_{c2}(0) = 0, \\
w_{c1}(1) &= \gamma_1 w_{b1}(s_1)\cos\theta, \\
w_{c2}(1) &= \gamma_2 w_{b2}(s_2)\cos\theta, \\
\left.\frac{\partial^3 w_{b1}}{\partial {x_i}^3}\right|_{x_i=0} &= -K_{T1}\, w_{b1}(0) \\
\left.\frac{\partial^2 w_{b1}}{\partial {x_i}^2}\right|_{x_i=0} &= K_{\theta 1}\left.\frac{\partial w_{b1}}{\partial x_i}\right|_{x_i=0} \\
\left.\frac{\partial^3 w_{b3}}{\partial {x_i}^3}\right|_{x_i=1} &= K_{T2}\, w_{b3}(1) \\
\left.\frac{\partial^2 w_{b3}}{\partial {x_i}^2}\right|_{x_i=1} &= -K_{\theta 2}\left.\frac{\partial w_{b3}}{\partial x_i}\right|_{x_i=1} \\
w_{b1}(s_1) = w_{b2}(s_1), &\left.\frac{\partial w_{b1}}{\partial x_i}\right|_{x_i=s_1} = \left.\frac{\partial w_{b3}}{\partial x_i}\right|_{x_i=s_2}, \\
&\left.\frac{\partial^2 w_{b1}}{\partial {x_i}^2}\right|_{x_1=s_1} = \left.\frac{\partial^2 w_{b2}}{\partial {x_i}^2}\right|_{x_i=s_2},
\end{aligned} \tag{17}$$

$$w_{b2}(s_2) = w_{b3}(s_2), \left.\frac{\partial w_{b2}}{\partial x_i}\right|_{x_i=s_2} = \left.\frac{\partial w_{b3}}{\partial x_i}\right|_{x_i=s_2},$$

$$\left.\frac{\partial^2 w_{b2}}{\partial {x_i}^2}\right|_{x_1=s_2} = \left.\frac{\partial^2 w_{b3}}{\partial {x_i}^2}\right|_{x_i=s_2},$$

$$\begin{aligned}
&\chi\left[\left.\frac{\partial^3 w_{b1}}{\partial {x_i}^3}\right|_{x_i=s_1} - \left.\frac{\partial^3 w_{b2}}{\partial {x_i}^3}\right|_{x_i=s_1}\right] \\
&\quad -\left(\sin\theta + \left.\frac{\partial y_1}{\partial x_i}\right|_{x_i=1}\cos\theta_1\right)\hat{e}_1 \\
&\quad -\frac{\cos\theta}{\mu}\left.\frac{\partial w_{c1}}{\partial x_i}\right|_{x_i=1} = 0, \\
&\chi\left[\left.\frac{\partial^3 w_{b2}}{\partial {x_i}^3}\right|_{x_i=s_2} - \left.\frac{\partial^3 w_{b3}}{\partial {x_i}^3}\right|_{x_i=s_2}\right] \\
&\quad -\left(\sin\theta + \left.\frac{\partial y_2}{\partial x_i}\right|_{x_i=1}\cos\theta_1\right)\hat{e}_2 \\
&\quad -\frac{\cos\theta}{\mu}\left.\frac{\partial w_{c2}}{\partial x_i}\right|_{x_i=1} = 0,
\end{aligned}$$

By analyzing Equations (14), their solutions can be expressed as follows:

$$\begin{aligned}
w_{bi}(x) = A_{ib}\cos\beta_b x + B_{ib}\sin\beta_b x \\
+ C_{ib}\cosh\beta_b x \\
+ D_{ib}\sinh\beta_b x \quad (i = 1,2,3)
\end{aligned} \tag{18}$$

$$w_{cj}(x) = E_{jc}\sin\beta_c x + F_{jc}\cos\beta_c x + D_{jc} \quad (j = 1,2)$$

In the equation above:

$$D_{jc} = \frac{8\mu d\hat{e}_j}{{\beta_c}^2} \tag{19}$$

By substituting Equation (18) into Equation (14), we arrive at:

$$\begin{aligned}
&\hat{e}_j = \tan\theta\left(E_{jc}\sin\beta_c + F_{jc}\cos\beta_c + D_{jc}\right) + \\
&\int_0^1 4d(1-2x_c)\beta_c(E_{jc}\cos\beta_c x - F_{jc}\sin\beta_c)dx_c \\
&= \left(sin\beta_c\tan\theta - 4d\left(sin\beta_c + \frac{2(cos\beta_c - 1)}{\beta_c}\right)\right)E_{jc} \\
&\quad + tan\theta D_{jc} \\
&\quad + \left(cos\beta_c tan\theta - 4d\left(1 + cos\beta_c - \frac{2sin\beta_c}{\beta_c}\right)\right)F_{jc}
\end{aligned} \tag{20}$$

The following equation provides an expression equivalent to Equation (19):

$$D_{jc} = \frac{8\mu d\hat{e}_j}{{\beta_c}^2} = \frac{8\mu d}{{\beta_c}^2 - 8\mu d tan\theta}\left(\hat{e}_j - tan\theta D_{jc}\right) \quad (21)$$

By substituting Equation (18) into Equation (20), we obtain:

$$D_{jc} = \eta_{j1c}E_{jc} + \eta_{j2c}F_{jc} \quad (22)$$

In the following equation:

$$\begin{aligned}\eta_{j1c} &= \frac{8\mu d}{{\beta_c}^2 - 8\mu d tan\theta} sin\beta_c tan\theta \\ &\quad - 4d\left(sin\beta_c + \frac{2(cos\beta_c - 1)}{\beta_c}\right) \\ \eta_{j2c} &= \frac{8\mu d}{{\beta_c}^2 - 8\mu d tan\theta}\left(cos\beta_c tan\theta\right. \\ &\quad \left. - 4d\left(1 + cos\beta_c - \frac{2sin\beta_c}{\beta_c}\right)\right) \\ &\quad (j = 1,2)\end{aligned} \quad (23)$$

3.2.2. Elastic Support

Integrating translational elastic supports into a suspended beam system represents a promising approach to enhancing the dynamic performance and versatility of suspended structures. The ability of elastic supports to absorb and dissipate energy, isolate vibrations, and exhibit nonlinear damping characteristics makes it a valuable addition to a wide range of engineering applications.

$$\frac{\partial^4 w_b(x)}{\partial x^4} + \beta^4 w_b(x) = 0 \quad (24)$$

The four remaining boundary conditions [25] at the intermediate elastic support at $x_1 = \mu \; and \; x_2 = \nu$ are:

$$\begin{aligned} & w_{bk}(x_i)|_{x_k=\mu} = w_{bk}(x_k)|_{x_k=\nu}, \\ & \left.\frac{dw_{bk}(x_k)}{dx_k}\right|_{x_k=\mu} = \left.\frac{dw_{bk}(x_k)}{dx_k}\right|_{x_k=\nu}, \\ & \left.\frac{d^2w_{bk}(x_k)}{dx_k^2}\right|_{x_k=\mu} = \left.\frac{d^2w_{bk}(x_i)}{dx_k^2}\right|_{x_k=\nu}, \\ & \left.\frac{d^3w_{bk}(x_k)}{{dx_k}^3}\right|_{x_k=\mu} = \left.\frac{d^3w_{bk}(x_k)}{{dx_k}^3}\right|_{x_k=\nu} \\ & \quad + K_{tk}w_{bk}(x_k)|_{x_k=\mu}, \\ & \quad (k = 1,2)\end{aligned} \quad (25)$$

Equation (24) is satisfied by the following expression for the deflections of the spans:

$$\begin{aligned} w_{bik}(x) &= A_k \cos\beta_i x + B_k \sin\beta_i x + C_k \cosh\beta_i x \\ &\quad + D_k \sinh\beta_i x \\ &\quad (k = 1,2,\dots,n)\end{aligned} \quad (26)$$

4. Comparative Study

4.1. Symmetric Cable-Stayed Beam

Based on the theoretical principles previously discussed in the formulation of the problem, by integrating the boundary conditions and continuity conditions of Equation (17) into Equations (18), a system of 16 linear equations is established. This system concerns the coefficients A_{ib}, B_{ib}, C_{ib}, D_{ib}, E_{jc} *and* F_{jc} where $(i = 1,2,3, j = 1,2)$. For this system to have a solution, the determinant of its coefficient matrix must be zero. This condition allows for the derivation of the characteristic equation of the combined structure, as shown in Equation (27).

$$[T]\{X\} = 0 \quad (27)$$

Within this configuration, the elements $t_{m,n}$ (where m and n take integer values between 1 and 16 inclusively) of the matrix, T correspond to the coefficients of the variables A_{ib}, B_{ib}, C_{ib}, D_{ib}, E_{jc}, F_{jc} where $(i = 1,2,3, j = 1,2)$ involved in the equations mentioned above.

The determination of the frequency ω is carried out by setting the determinant of the coefficient matrix $[T]$ to zero. By using the Newton-Raphson method to determine the frequency ω, the vector of coefficients is easily obtained by combining it with the boundary conditions. The mode shapes of each order then result from this determination.

The representation of the vibration modes of a beam is achieved using piecewise functions, such as:

$$\begin{aligned} w_{bi}(x) &= A_{ib}\cos\beta_b x_i + B_{ib}\sin\beta_b x_i \\ &\quad + C_{ib}\cosh\beta_b x_i + D_{ib}\sinh\beta_b x_i \\ & s_{i-1} < s_i < s_1, s_1 = 0, s_3 = 1, \\ & (i = 1,2,3)\end{aligned} \quad (28)$$

Taking practical engineering constraints into account, the following physical parameters have been selected.

To validate the theory presented in this article, a double cable-stayed beam model was developed using a computational program, employing the same parameters as those used in studies conducted in the literature. In addition to the previous work on the simply supported beam case, the present study includes the Clamped-Clamped (CC) and Clamped-Simply supported (CS) beam cases.

Table 1. Physical parameters (cable and beam)

Cable		Beam	
Material	CFRP (Carbon Fiber Reinforced Polymer)	**Type**	Box-Girder Beam in Reinforced Concrete
Linear Mass (kg/m)	10,4	**Linear Mass (kg/m)**	$4{,}4 * 10^4$
Cross-Sectional Area (m^2)	$6{,}273 * 10^{-3}$	**Cross-Sectional Area (m^2)**	16,3
Elastic Modulus (GPa)	210	**Elastic Modulus (GPa)**	34,5
Initial Force (MN)	1	**Moment of Inertia of the Section (m^4)**	9,8
Inclination Angle (degree)	30	**Length (m)**	300

Table 2. Comparison of the first six natural frequencies of double cable-stayed beams in SS, CS, and CC cases

Natural Frequency	1st	2nd	3rd	4th	5th	6th	K_{T1}	K_{T2}	$K_{\theta 1}$	$K_{\theta 2}$
Present Study (SS)	0,1362	0,2310	0,4354	0,7849	1,2162	1,3428	0	0	0	0
Theoretical Value (SS) [2]	0,1355	0,2307	0,4354	0,7848	1,2162	1,3503				
ANSYS (SS) [2]	0,1360	0,2307	0,4349	0,7840	1,2147	1,3436				
Present Study (CC)	0,1680	0,3370	0,5940	0,9850	1,4700	2,0440	∞	∞	∞	∞
Present Study (CS)	0,1480	0,2770	0,5140	0,8810	1,3360	1,3420	∞	0	∞	0

A numerical approach was implemented in MATLAB to solve the system of equations resulting from the imposed boundary and continuity conditions. The iterative Newton-Raphson method was used for this purpose.

Using the same parameters as those defined in previous studies reported in the literature, Table 2 presents a comparison between the first six natural frequencies of a cable-stayed beam, obtained by applying the theory presented in this article, and those derived from numerical simulations performed with the finite element model mentioned in the literature.

Table 2 provides a detailed analysis of the different cases comparing the frequency values obtained in this study with those referenced in sources [2], thereby highlighting the accuracy of recent data. The results demonstrate exceptional consistency, with negligible errors regarding the frequencies of the first ten modal shapes. This finding indicates that the analytical methods and strategies employed in this research are robust, offering results that are not only precise but also consistent with recognized knowledge in this field of study.

The configuration of a beam's supports significantly impacts its natural frequencies. These frequencies represent the inherent vibrational modes of the beam and are crucial for understanding its dynamic behavior. Three main configurations are typically analyzed: Simply Supported (SS), Clamped-Clamped (CC), and Clamped-Simply supported (CS):

- Simply Supported (SS): In this configuration, both ends of the beam are free to rotate and translate. This minimal constraint allows for the most significant bending deformation, resulting in the lowest natural frequencies among the three configurations. The absence of fixity minimizes the beam's stiffness, leading to lower energy barriers for vibration and, consequently, lower frequencies.
- Clamped-Clamped (CC): Conversely, the CC configuration features both ends of the beam fixed, completely preventing any rotational or translational movement. This fixed-end condition offers the maximum level of constraint, significantly increasing the beam's overall stiffness. The higher stiffness translates to a greater energy requirement to initiate vibration, leading to the highest natural frequencies observed in the three configurations.
- Clamped-Simply Supported (CS): The CS configuration presents an intermediate case between SS and CC. One end of the beam is fixed, providing substantial stiffness, while the other end is simply supported, allowing for some degree of rotation and translation. This combination results in natural frequencies that are higher than those of the SS configuration but lower than those of the CC configuration. The clamped end offers significant constraint, but the simply supported end allows for some modal flexibility, resulting in a compromise between the two extreme cases.

The natural frequencies of the cable-stayed beam vary significantly based on the support conditions. The SS configuration exhibits the lowest natural frequencies due to minimal constraints, the CC configuration shows the highest natural frequencies owing to maximum constraints, and the CS configuration falls in between. Understanding these variations is crucial for designing and analyzing the dynamic behavior of cable-stayed beams in different structural applications.

The first four mode shapes are essential (Figure 3). We present these primary shapes to enhance understanding and facilitate the comparison of their behavior.

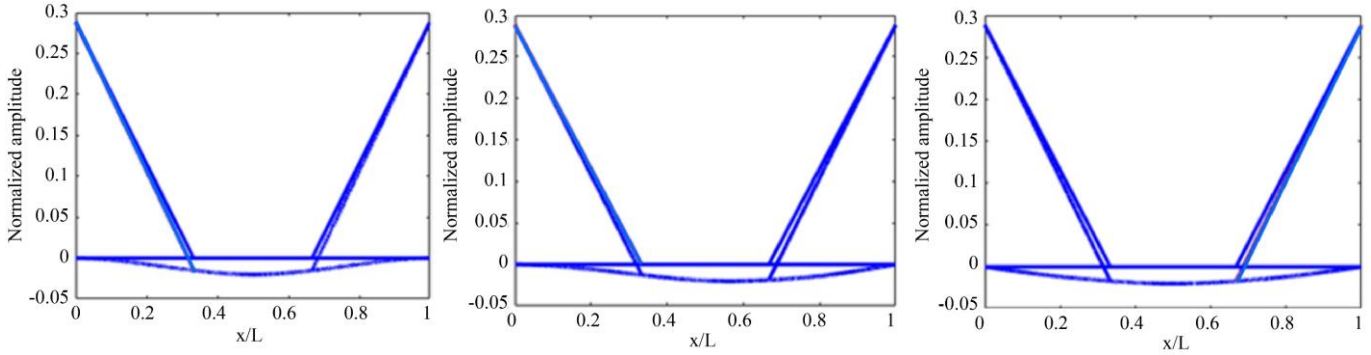

(a-1) The 1st order mode (CC) **(b-1) The 1st order mode (CS)** **(c-1) The 1st order mode (SS)**

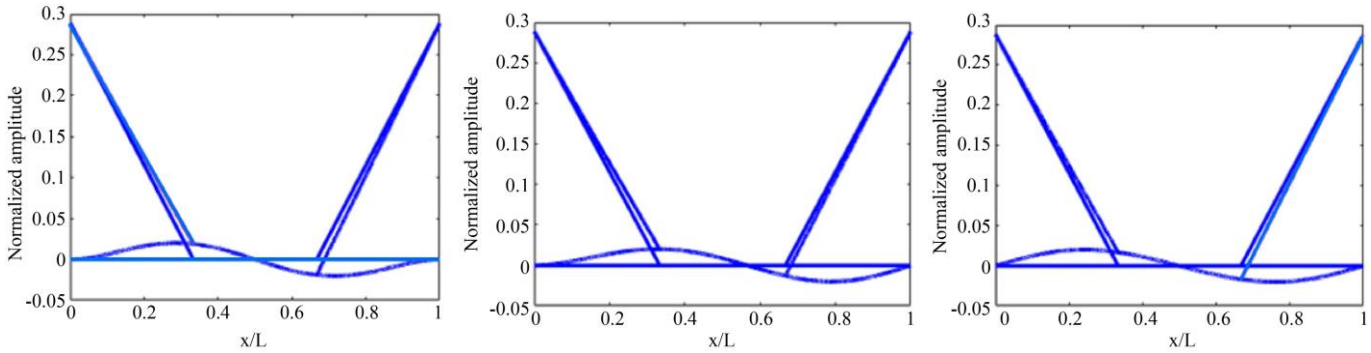

(a-2) The 2nd order mode (CC) **(b-2) The 2nd order mode (CS)** **(c-2) The 2nd order mode (SS)**

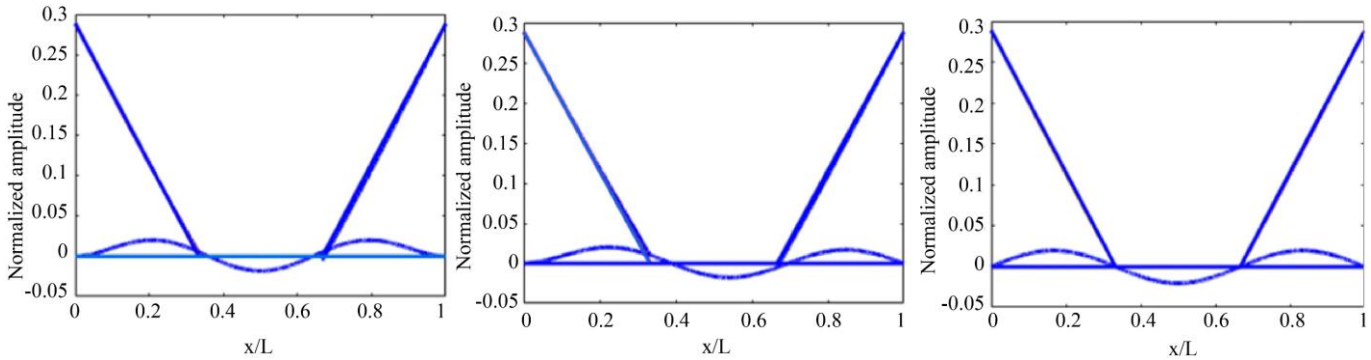

(a-3) The 3rd order mode (CC) **(b-3) The 3rd order mode (CS)** **(c-3) The 3rd order mode (SS)**

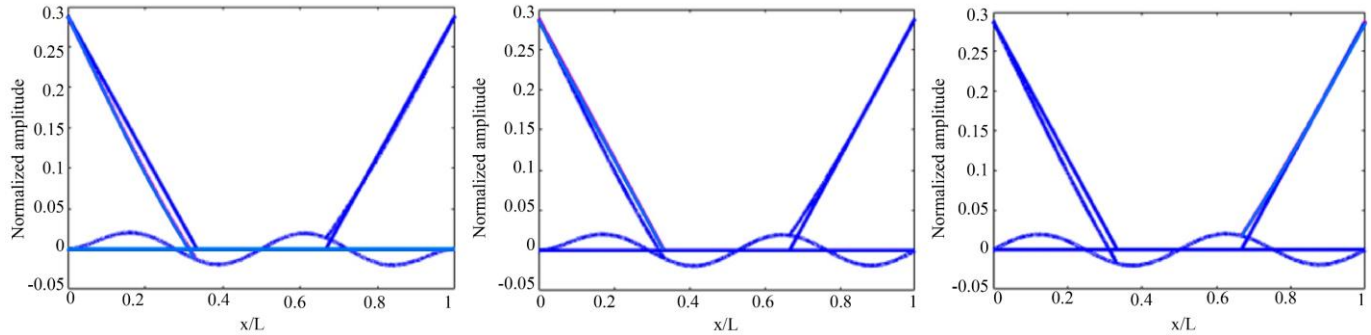

(a-4) The 4th order mode (CC) **(b-4) The 4th order mode (CS)** **(c-4) The 4th order mode (SS)**

Fig. 3 The first 4 mode shapes of a double cable-stayed beam

The parametric analysis of the modal behaviors of the double cable-stayed beam model, particularly with regard to the studied configurations, provides a valuable tool for the design and analysis of these structures. By understanding the influence of support conditions on natural frequencies and vibration modes, engineers can optimize the dynamic performance of double cable-stayed beams and ensure their structural integrity under various loads.

Understanding the variations in natural frequencies based on support configurations is crucial for the optimal design of double cable-stayed beams. By carefully selecting the support conditions, engineers can:

- Achieve the desired natural frequencies for the structure.
- Avoid potential resonance issues.
- Optimize the dynamic performance of the beam.
- Ensure the safety and reliability of the structure under different loading conditions.

4.2. Analysis of Calculation Examples

The impact of flexural rigidity on structural frequencies is depicted in Figure 4. This analysis of axial rigidity and flexural rigidity will be applied to a cable-beam system with a simply supported beam. A general trend of increasing frequencies across all modes with rising flexural rigidity is observed, particularly evident for higher-order modes. This relationship can be attributed to the concomitant increase in the moment of inertia I_b of the cross-section with flexural rigidity, enhancing the structure's resistance to deformation. By holding the modulus of elasticity constant, the effect of flexural rigidity on frequencies can be examined in detail.

The findings reveal a proportional rise in the frequencies of various modes with increasing flexural rigidity. This observation holds particular significance for vibration-prone structures, as high frequencies can substantially impact structural stability and performance. In cases where the moment of inertia I_b of the cross-section is considerably low, both flexural rigidity and the relative axial rigidity of the member are also diminished. This scenario leads to a decrease in the frequencies of all modes, potentially rendering the structure more susceptible to vibrations.

When analyzing a beam as a simple continuous beam with two supports, a direct relationship between its flexural rigidity and the frequencies of its vibration modes becomes evident. Higher flexural rigidity corresponds to an increase in frequencies.

However, this relationship is not strictly linear. In scenarios where the moment of inertia I_b of the cross-section is substantial, the beam's flexural rigidity experiences a significant rise, while the relative axial rigidity of the member remains comparatively low. This disparity mitigates the impact of beam rigidity on frequencies, consequently slowing down the growth of the frequency curves.

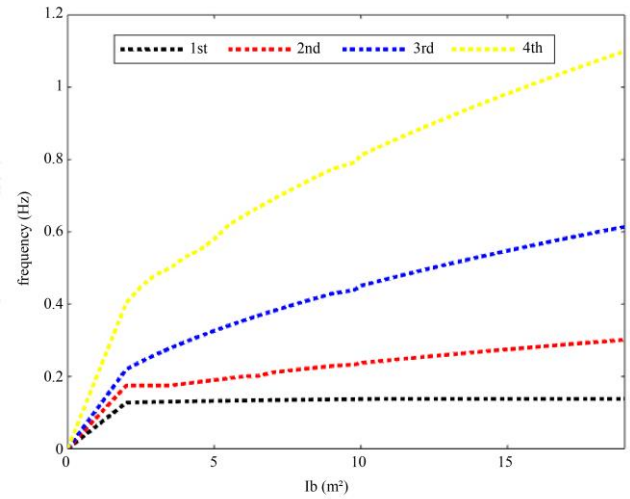

Fig. 4 Effect of beam flexural rigidity on the system's first four frequencies

This effect is particularly prominent for the frequencies associated with the lower vibration modes of the structure. This implies that slower vibration modes exhibit greater sensitivity to variations in flexural rigidity compared to faster vibration modes.

In practical engineering projects, it is crucial to account for this phenomenon, as it can potentially lead to vibration issues within structures. Therefore, particular attention should be paid to flexural rigidity, especially for structures prone to significant vibrations.

The analysis depicted in Figure 5 explores the impact of the axial rigidity of a tension member on the first four natural frequencies of a structural system. Utilizing the exceptional properties of Carbon Fiber-Reinforced Polymer (CFRP) materials, known for their lightweight nature, high strength, and a wide range of adjustable elasticity moduli, the study maintains a constant cross-section for the tension member while varying its axial rigidity by adjusting the elasticity modulus. As the analysis reveals, a progressive increase in the axial rigidity of the tension member translates into a gradual elevation of the frequencies of the system's various modes.

Unlike the observation made in Figure 4, where the influence was primarily concentrated on lower-order vibration modes, the enhancement of axial rigidity leads to an overall increase in system stiffness, manifested by a rise in the frequencies of higher-order modes. Interestingly, the third natural frequency of the system remains virtually unchanged.

This behavior can be attributed to the fact that the third mode, corresponding to a global bending mode, is less sensitive to variations in the axial rigidity of the tension member and consequently has minimal impact on the overall dynamic characteristics of the system.

The analysis sheds light on the intricate relationship between beam flexural rigidity and tension member axial rigidity in relation to structural safety. On the one hand, increasing the beam's flexural rigidity tends to diminish the influence of the member's axial rigidity and amplify the stress jump. On the other hand, as illustrated in Figure 4, the frequencies of each mode of the structure elevate with increasing beam flexural rigidity.

This frequency increase is accompanied by a rise in the modal energies of each mode, resulting in enhanced transmission of axial energy and an exacerbation of structural safety concerns. Consequently, it is crucial to control beam flexural rigidity within reasonable limits to prevent fatigue issues due to high-frequency vibrations and ensure the structural safety of the beam.

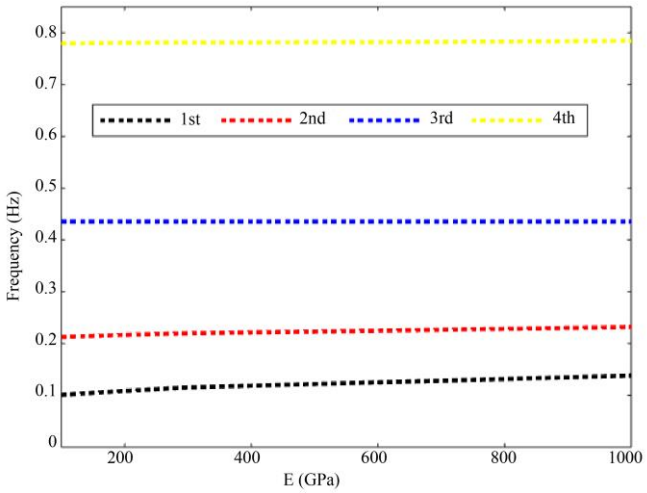

Fig. 5 Effect of beam axial rigidity on the system's first four frequencies

The judicious utilization of CFRP materials with high elasticity and high strength can significantly improve the axial rigidity of tension members, thereby augmenting their capacity to withstand vibrations and deformations. Moreover, the enhancement of axial rigidity leads to a reduction of internal stresses within the beam, which diminishes the effects of bending on the supports of the tension member and decreases the shear forces borne by the beam.

In summary, the analysis highlights the predominant influence of axial rigidity on natural frequencies and the structural safety of a beam. The employment of CFRP materials proves to be an effective solution for enhancing the axial rigidity of tension members and reinforcing the overall structural safety of the system.

This section of the study is essential for demonstrating and validating the employed method as well as the chosen mathematical formulation. It aims to justify the use of this approach to address more concrete situations, particularly the analysis of beams supported by elastic supports, a common configuration in engineering. Elastic supports with varying stiffness and positioning represent these supports.

5. Case Numerical Results and Discussions

5.1. Case of Double Cable-Stayed Beam Supported by a Single Elastic Support

A parametric study is conducted to evaluate the effectiveness of supports in reducing the structural vibrations of a cable-stayed beam. The objective is to determine the optimal positions of the supports to maximize structural stability. The proposed method relies on the demonstration of its accuracy and reliability through simplified cases, as described in previous references and comparisons.

The application to more complex and practical cases is envisaged, with the aim of providing precise recommendations for the design and optimization of structures that minimize vibrations and maximize durability and safety. The continuation of this study involves examining a cable-beam system with a simply supported beam.

5.1.1. Parametric Study of a Double Cable-Stayed Beam, Supported by an Elastic Support Located at the Midpoint of the Beam with a Variable Stiffness

The case under study involves a cable-stayed beam that is simply supported at both ends and supported by elastic supports with stiffness K_{t1} placed in the middle of the beam (x = 0.5L). The dimensionless stiffness values range from 0 to 1000. A parametric analysis is performed to determine the optimal position of the support that minimizes the beam's vibrations.

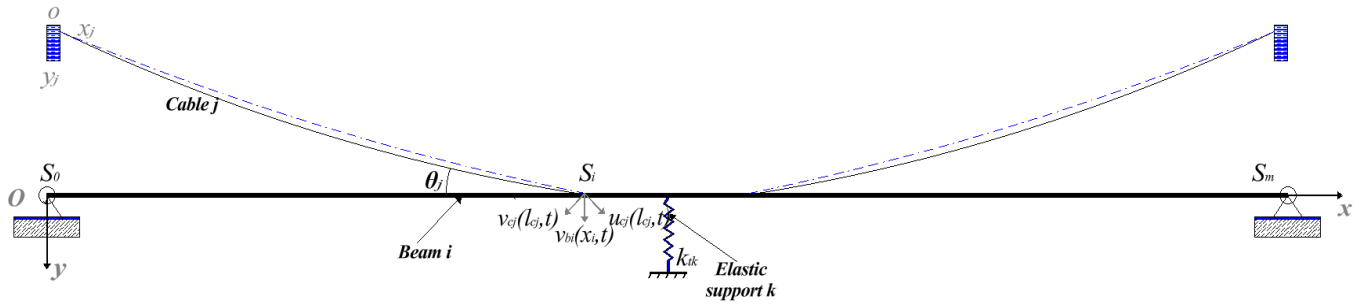

Fig. 6 Configurations of a double cable-stayed beam supported by a single elastic support

Table 3. Analysis of the first four natural frequencies of a double cable-stayed beam, supported by an elastic support with stiffness K_{t1} located at the midpoint of the beam

Stiffness	Frequencies			
	Mode 1	Mode 2	Mode 3	Mode 4
0	5,269409	6,845584	9,348907	12,592821
10	5,309370	6,845800	9,356735	12,592884
50	5,458432	6,846774	9,388008	12,593060
100	5.622701	6.819242	9.387941	12.573431
200	9,726650	12,595811	15,646078	18,622535
1000	10,090200	12,599359	15,646078	18,622535

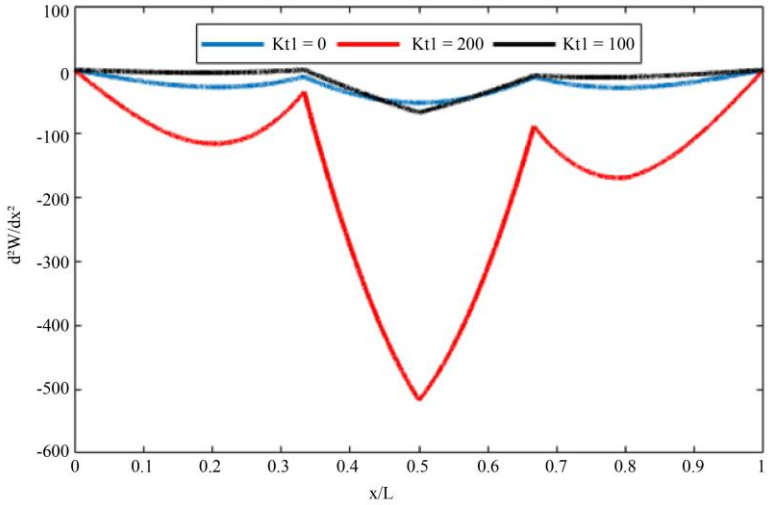

Fig. 7 Curvatures corresponding to the deflection shapes of a simply supported beam with an elastic support located at $x_1 = 0.5L$ for different stiffnesses

In contrast to the first case examined in this study, the frequencies analyzed in this segment are dimensionless. The analysis reveals that as the value of the dimensionless stiffness increases, the natural frequencies of the four modes also increase. This result is significant because the elastic support adds stiffness to the system, thereby enhancing the overall rigidity of the structure.

This increase in natural frequencies can be explained by the effect of the elastic support modeled by a translational elastic support placed in the middle of the beam. This support helps to reduce the amplitude of the vibrations. The decrease in amplitude leads to an increase in frequency, as the beam tends to vibrate at a higher frequency.

Figure 7 demands an analysis of the curvatures based on the different stiffnesses of the elastic supports:

- Black Curve ($K_{t1} = 100$): Minimal curvature at the center and support points, indicating minimal beam deflection. High support rigidity significantly reduces deflection, enhancing structural stability.
- Red Curve **($K_{t1} = 200$):** More pronounced curvature compared to the black curve, but still controlled. Moderate support rigidity balances flexibility and stability, allowing controlled deformations while maintaining structural stiffness.
- Blue Curve **($K_{t1} = 0$):** Most pronounced curvature, with high peaks at support points and maximum deflection at the center. The absence of support rigidity allows maximum deflection, which can be detrimental to structural stability.

The results align with structural mechanics principles. Increased support rigidity reduces deflection and enhances overall stiffness, as expected. The curves clearly demonstrate the influence of support rigidity levels on beam deflections, validating theoretical principles. The study of the variation of the first four dimensionless natural frequencies as a function of the linear stiffness of the translational elastic support, located at a position of $x = 0.5L$, allows for a better understanding of the influence of elastic supports on the natural frequencies of a cable-stayed beam.

5.1.2. Parametric Study of a Double Cable-Stayed Beam, Supported by an Elastic Support with a Variable Position

The following methodology adopted involves placing the elastic support at different points along the beam, systematically varying its position.

For each position of the elastic support, an analysis is performed to determine the natural frequencies of the four modes of vibration.

Table 4. Analysis of the first four natural frequencies of a beam-stayed cable supported by an elastic support with a stiffness of $K_{t1} = 100$, as a function of the elastic support position

Position of Elastic Support	Frequencies			
	Mode 1	Mode 2	Mode 3A	Mode 4
0,25	9,342073	12,566342	15,711134	18,677227
1/3	5,816707	6,736405	9,298534	12,550414
0,5	5,458432	6,846774	9,388008	12,593060
2/3	5,478216	6,953659	9,299228	12,596901
0,75	5,409283	7,001665	9,346102	12,573411

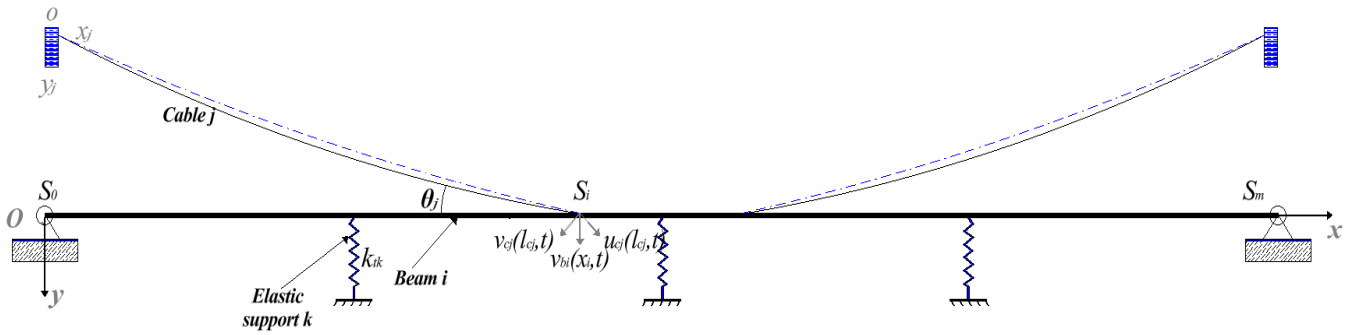

Fig. 8 Configurations of a double cable-stayed beam supported by multiple (two/three) elastic supports

This result underscores the importance of structural stiffness in controlling vibrations. By increasing the stiffness of a structure, its natural frequencies can be elevated, shifting them out of the range of common excitation frequencies. This helps to minimize the risks of resonance and improve the overall vibrational performance of the structure.

5.2. Case of a Double Cable-Stayed Beam Supported by Multiple Elastic Supports

After examining the two scenarios of a double cable-stayed beam supported by elastic support, where we varied the stiffness and position of the elastic support, it is essential to highlight that the first analysis focused on a simplified case with a single elastic support. However, in practical applications, structures may involve multiple support schemes, which complicate their dynamic behavior. Thus, to achieve designs that optimally meet practical requirements, it is crucial to conduct more in-depth analyses that consider these multiple support configurations.

This configuration allows us to explore how the variation in the stiffness coefficients of these elastic supports influences the vibrational behavior of the beam.

The primary objective is to determine how these variations affect the natural frequencies and modes of vibration of the beam, thereby providing crucial data for the development of more robust design solutions that are well-suited to the real-world constraints of engineering structures.

5.2.1. Parametric Study of a Double Cable-Stayed Beam, Supported by Two Elastic Supports with Variable Stiffness

The following section of the study extends this approach by examining the behavior of a double cable-stayed beam supported by two elastic supports positioned symmetrically at relative positions of 1/3 and 2/3 of the beam's length ($L_1/L = 1/3$ and $L_3/L = 2/3$).

Table 5. Analysis of the first four natural frequencies of a cable-stayed beam supported by two elastic supports with stiffness K_{t1} and K_{t3}, positioned at L1/L = 1/3 and L3/L = 2/3, respectively

Stiffness	Frequencies			
	Mode 1	Mode 2	Mode 3	Mode 4
$K_{t1} = 0, K_{t3} = 0$	5,26245	6,81466	9,29756	12,57275
$K_{t1} = 10, K_{t3} = 0$	5,27150	6,83003	9,30692	12,57497
$K_{t1} = 100, K_{t3} = 100$	5,35015	6,96964	9,39601	12,59705
$K_{t1} = 10, K_{t3} = 1000$	5,58825	7,65164	10,04704	12,85459
$K_{t1} = 100, K_{t3} = 100$	5,42587	7,08082	9,46714	12,61648
$K_{t1} = 10000, K_{t3} = 1000$	6,55999	10,27423	13,62499	15,71113

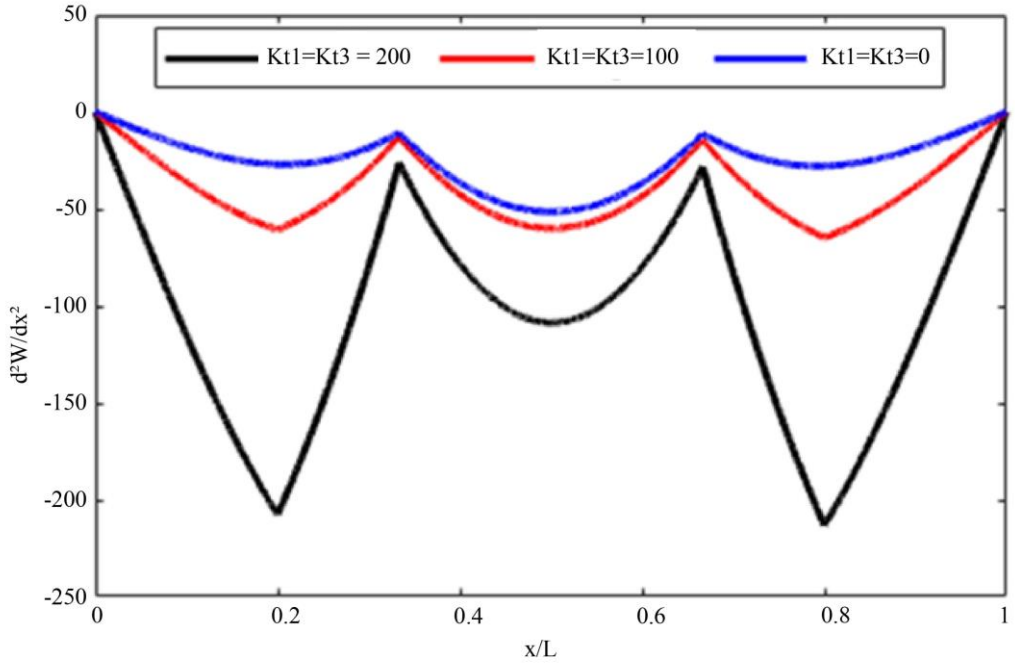

Fig. 9 Curvatures corresponding to the deflection shapes of a simply supported beam with two elastic supports located at $x_1 = 0.5L$ and $x_2 = 0.8L$ for different stiffnesses

Table 5 illustrates the dimensionless natural frequencies of a beam supported by two elastic supports placed symmetrically at positions($L_1/L = 1/3$ and $L_3/L = 2/3$). When adjusting the stiffness coefficients of these elastic supports, a notable variation in the frequencies is observed. This analysis reveals that increasing the stiffness of the elastic supports makes the structure more rigid. This increase in rigidity is attributable to the parallel arrangement of the elastic supports, where the total stiffness equals the sum of the stiffnesses of each elastic support. This aligns with the conclusions from Table 3, which indicated an increase in the structure's frequency as the stiffness of the elastic supports supporting the beam increased.

Figure 9 requires a careful interpretation for a thorough analysis of the curvatures for different stiffnesses of the elastic supports:

- Black Curve **($K_{t1} = K_{t3} = 200$):** The curvature is the lowest at the middle and support points, indicating minimal deflection of the beam. The high stiffness of the supports significantly reduces deflection, thereby increasing the overall rigidity of the structure. High support stiffness reduces deformations, which is beneficial for structures requiring increased stability.
- Red Curve **($K_{t1} = K_{t3} = 100$):** The curvature is slightly more pronounced than in the previous case but remains significantly controlled compared to lower stiffnesses. Moderate support stiffness provides a balance between flexibility and stability, allowing for controlled deformations while maintaining good structural rigidity.
- Blue Curve **($K_{t1} = K_{t3} = 0$):** The curvature is the most pronounced, showing higher peaks at the support points and greater deflection in the middle. This indicates that the beam undergoes maximum deformation in the absence of support stiffness. The absence of support stiffness allows for maximum deflection, which may be undesirable for applications requiring structural stability.

The presented results are in agreement with structural mechanics theories. Higher support stiffness leads to reduced deflection and increased overall structural rigidity, as expected. The curves consistently demonstrate how different levels of support stiffness influence the beam's deflection shapes. Therefore, the results are logical and validated by theoretical principles.

5.2.2. Parametric Study of a Double Cable-Stayed Beam, Supported by Three Elastic Supports with Variable Stiffness

It is essential to conclude the study with an analysis of the dimensionless natural frequencies of a beam supported by three elastic supports: a central elastic support and two others placed symmetrically at the points $L_1/L = 1/3$ and $L_3/L = 2/3$. The dimensionless stiffness of the elastic support located at the center is set to $K_{t2} = 100$.

Table 6. Analysis of the first four natural frequencies of a cable-stayed beam supported by three elastic supports with stiffness K_{t1}, K_{t2} and K_{t3}, positioned at $L_1/L = 1/3, L_2/L = 1/2$, and $L_3/L = 2/3$, respectively, where $K_{t2} = 100$

Stiffness	Frequencies			
	Mode 1	Mode 2	Mode 3	Mode 4
$K_{t1} = 0, K_{t3} = 0$	5,62270	6,81924	9,38794	12,57343
$K_{t1} = 10, K_{t3} = 0$	5,63097	6,83424	9,39606	12,57565
$K_{t1} = 100, K_{t3} = 100$	5,69748	6,97587	9,47390	12,59775
$K_{t1} = 10, K_{t3} = 1000$	5,88505	7,69239	10,08201	12,85459
$K_{t1} = 100, K_{t3} = 100$	5,76966	7,08289	9,53829	12,61713
$K_{t1} = 10000, K_{t3} = 1000$	6,96761	10,27668	13,62551	15,71120

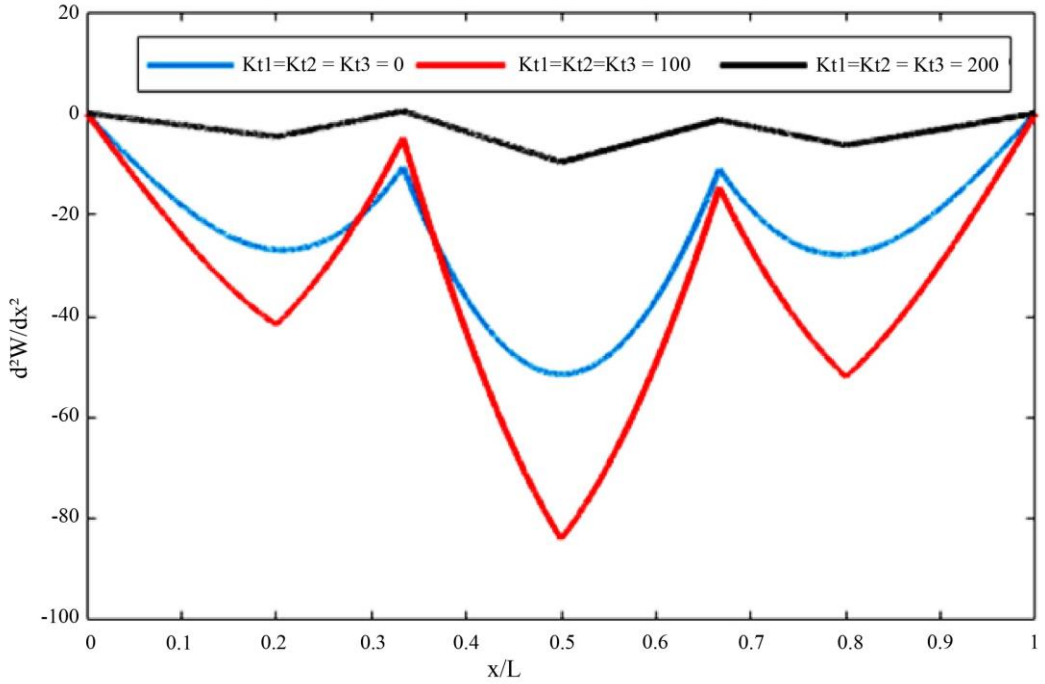

Fig. 10 Curvatures corresponding to the deflection shapes of a simply supported beam with three elastic supports located at $x_1 = 0.2L$, $x_2 = 0.5L$ and $x_3 = 0.8L$ for different stiffnesses

Adjusting the stiffness coefficients of these elastic supports results in notable variations in the frequencies. Analysis of these data reveals that increasing the stiffness of the elastic supports makes the overall structure more rigid. This increase in rigidity is primarily due to the central elastic support, which increases the total stiffness of the beam in its middle, functioning as a concentrated support. These results are consistent with those presented in Table 3, which indicated a rise in the structure's frequency corresponding to the increased stiffness of the support elastic supports.

Figure 10 requires careful interpretation for a thorough analysis of curvatures for different elastic support stiffnesses; the results follow the same logic as the case of a beam simply supported by two elastic supports. Increasing the stiffness of the elastic supports (from 0 to 200) reduces the deflection of the beam, thus increasing the overall rigidity of the structure. This is evident from the decrease in curvature in the black and red curves compared to the blue curve.

Elastic support points create stress points where the curvature can change significantly. With varying stiffnesses, the transition between elastically supported beam segments and unsupported segments is more or less pronounced.

This section presents a modal analysis of the cable-stayed beam, focusing on the first two linear modes. The aim is to investigate how the configuration of the elastic supports influences the structural vibration behavior. The following illustrations depict the vibration modes of the beam under three different arrangements.

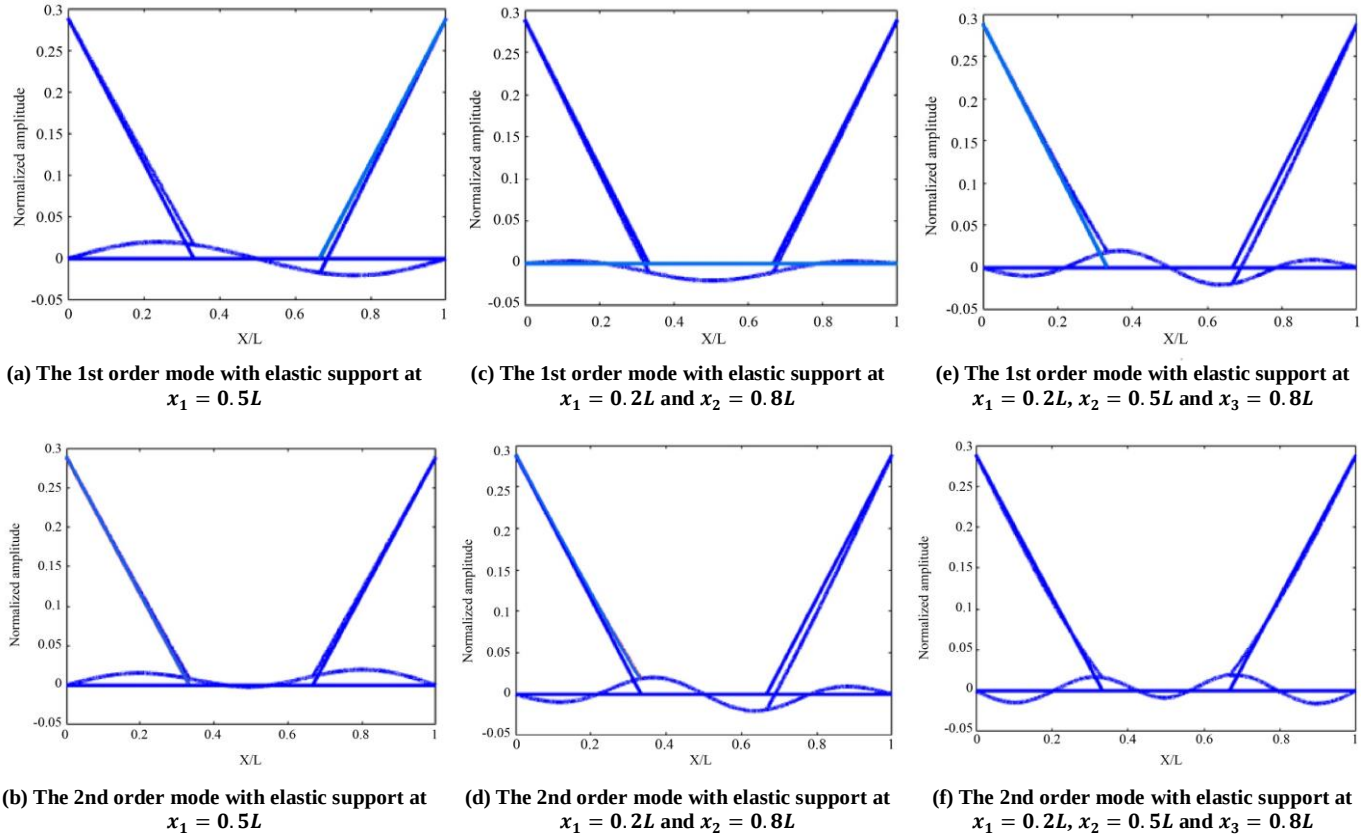

(a) The 1st order mode with elastic support at $x_1 = 0.5L$

(c) The 1st order mode with elastic support at $x_1 = 0.2L$ and $x_2 = 0.8L$

(e) The 1st order mode with elastic support at $x_1 = 0.2L$, $x_2 = 0.5L$ and $x_3 = 0.8L$

(b) The 2nd order mode with elastic support at $x_1 = 0.5L$

(d) The 2nd order mode with elastic support at $x_1 = 0.2L$ and $x_2 = 0.8L$

(f) The 2nd order mode with elastic support at $x_1 = 0.2L$, $x_2 = 0.5L$ and $x_3 = 0.8L$

Fig. 11 Illustration of the first two linear modes of a beam incorporating cables and elastic supports. The diagrams on the left (a, b) correspond to a configuration where the beam is supported by a single elastic support located at x=0.5Lx = 0.5Lx= $0.5L$. The diagrams in the center (c, d) depict the beam supported by two elastic supports located at $x_1 = 0.2L$ and $x_2 = 0.8L$. The diagrams on the right (e, f) correspond to a configuration where the beam is supported by three elastic supports located at $x_1 = 0.2L$, $x_2 = 0.5L$ and $x_3 = 0.8L$.

The figures above present complex data that requires careful analysis and detailed description to facilitate comprehension. Here is a structured analysis of the observations and implications of these figures:

- Mode (a) and (b): The presence of a single elastic support modifies the vibration modes by concentrating the amplitudes at the support point.
- Mode (c) and (d): The presence of two elastic supports distributes the amplitudes more evenly along the beam, reducing deformations at the support points.
- Mode (e) and (f): The presence of three elastic supports increases the overall stiffness of the beam, reducing the maximum amplitudes and distributing the nodes more regularly.

The results from the figures clearly demonstrate the influence of the elastic support configuration on the beam's vibration modes. Adding elastic supports increases the beam's stiffness, which translates into reduced vibration amplitudes at the support points. Evenly distributed supports along the beam help to distribute loads and deformations more homogeneously.

The analysis of the vibration modes of the cable-stayed beam with elastic supports highlights the importance of support configuration in controlling the structure's vibration behaviors. By adjusting the position and stiffness of the supports, it is possible to optimize the dynamic performance and stability of the beam, thus offering effective solutions for various engineering applications.

6. Conclusion

This research focused on analyzing the transverse vibrations of a cable-stayed beam resting on elastic supports within a linear framework. The differential equation governing the beam's vibrational behavior was solved under different configurations, and the obtained natural frequencies demonstrated consistency with existing literature data.

Validation of these results was ensured through a meticulous convergence analysis of natural frequencies, as well as thorough comparisons between the employed method, the Finite Element Method (FEM), and experimental approaches, thus demonstrating the robustness of the employed technique.

Parametric studies were conducted on double-cabled beams with one or multiple elastic supports (two and three springs), revealing significant variations in the vibrational response. These variations highlight the importance of these factors in structural design and pave the way for further research on the optimization of cable-stayed structures.

The study also explored the significant impact of various factors, such as the stiffness, number, and position of elastic supports, on vibration suppression effectiveness. The results revealed that increasing the stiffness of elastic supports makes the overall structure more rigid, thereby minimizing the risk of resonance and enhancing the overall vibrational performance of the structure.

In conclusion, while this study focused on a linear approach, an extension to investigating the same system in a nonlinear context could offer even deeper insights into the dynamic behavior of cable-stayed structures. This extension would allow for better exploitation of the obtained results and significantly contribute to the design and optimization of these systems in practical applications. The adaptability and efficiency of the presented method show considerable potential for specific adjustments to real-world structures, thus enhancing their durability and functionality in various engineering contexts. Furthermore, incorporating elastomeric bearings into the design can greatly enhance the dynamic performance and longevity of these structures by effectively managing vibrational characteristics.

Acknowledgments

This research was made possible by the generous support of the High School of Technology of Casablanca, the National School of Electricity and Mechanics of Casablanca, and Hassan II University of Casablanca.

References

[1] Yunyue Cong et al., "Modeling, Dynamics, and Parametric Studies of a Multi-Cable-Stayed Beam Model," *Acta Mechanic*, vol. 231, no. 12, pp. 4947-4970, 2020. [CrossRef] [Google Scholar] [Publisher Link]

[2] Yunyue Cong et al., "A Multiple Cable-Beam Model on in-Plane Free Vibration of Cable-Stayed Bridge with CFRP Cables and Modal Analysis," *Journal of Dynamics and Control*, vol. 15, no. 6, pp. 494-504, 2017. [CrossRef] [Publisher Link]

[3] Tieding Guo et al., "Nonlinear Vibrations for Double Inclined Cables–Deck Beam Coupled System Using Asymptotic Reductions," *International Journal of Non-Linear Mechanics*, vol. 108, pp. 33-45, 2019. [CrossRef] [Google Scholar] [Publisher Link]

[4] Xiaoyang Su et al., "Dynamic Analysis of the In-Plane Free Vibration of a Multi-Cable-Stayed Beam with Transfer Matrix Method," *Archive of Applied Mechanics*, vol. 89, pp. 2431-2448, 2019. [CrossRef] [Google Scholar] [Publisher Link]

[5] Kang Houjun, Cong Yunyue, and Su Xiaoyang, "Cable-stayed Shallow-arch Modeling and In-Plane Free Vibration Analysis of Cable-stayed Bridge with CFRP Cables," *Chinese Journal of Solid Mechanics*, vol. 39, no. 3, pp. 316-327, 2018. [CrossRef] [Google Scholar] [Publisher Link]

[6] Yunyue Cong, Houjun Kang, and Tieding Guo, "Planar Multimodal 1:2:2 Internal Resonance Analysis of Cable-Stayed Bridge," *Mechanical Systems and Signal Processing*, vol. 120, pp. 505-523, 2019. [CrossRef] [Google Scholar] [Publisher Link]

[7] D.Q. Cao et al., "Modeling and Analysis of the In-Plane Vibration of a Complex Cable-Stayed Bridge," *Journal of Sound and Vibration*, vol. 331, no 26, pp. 5685-5714, 2012. [CrossRef] [Google Scholar] [Publisher Link]

[8] Xiaoyang Su et al., "Modeling and Parametric Analysis of In-Plane Free Vibration of a Floating Cable-Stayed Bridge with Transfer Matrix Method," *International Journal of Structural Stability and Dynamics*, vol. 20, no. 1, 2020. [CrossRef] [Google Scholar] [Publisher Link]

[9] Rujin Ma, Xinzhong Chen, and Airong Chen, "Effect of Cable Vibration on Aerostatic Response and Dynamics of a Long Span Cable-Stayed Bridge," *New Horizons and Better Practices*, pp. 1-10, 2007. [CrossRef] [Google Scholar] [Publisher Link]

[10] C. Gentile, and F. Martinez y Cabrera, "Dynamic Performance of Twin Curved Cable-Stayed Bridges," *Earthquake Engineering Structural Dynamics*, vol. 33, pp. 15-34, 2004. [CrossRef] [Google Scholar] [Publisher Link]

[11] Xiaoyang Su et al., "Internal Resonance and Energy Transfer of a Cable-Stayed Beam with a Tuned Mass Damper," *Nonlinear Dynamics*, vol. 110, pp. 131-152, 2022. [CrossRef] [Google Scholar] [Publisher Link]

[12] Yunyue Cong, and Houjun Kang, "Planar Nonlinear Dynamic Behavior of a Cable-Stayed Bridge under Excitation of Tower Motion," *European Journal of Mechanics - A/Solids*, vol. 76, pp. 91-107, 2019. [CrossRef] [Google Scholar] [Publisher Link]

[13] Jian Peng et al., "Nonlinear Primary Resonance in Vibration Control of Cable-Stayed Beam with Time Delay Feedback," *Mechanical Systems and Signal Processing*, vol. 137, 2020. [CrossRef] [Google Scholar] [Publisher Link]

[14] J. Zhu et al., "Dynamic Behavior of Cable-Stayed Beam with Localized Damage," *Journal of Vibration and Control*, vol. 17, no. 7, pp. 1080-1089, 2011. [CrossRef] [Google Scholar] [Publisher Link]

[15] Yunyue Cong, Houjun Kang, and Guirong Yan, "Investigation of Dynamic Behavior of a Cable-Stayed Cantilever Beam under Two-Frequency Excitations," *International Journal of Non-Linear Mechanics*, vol. 129, 2021. [CrossRef] [Google Scholar] [Publisher Link]

[16] Yunyue Cong et al., "One-to-One Internal Resonance of a Cable-Beam Structure Subjected to a Concentrated Load," *Journal of Sound and Vibration*, vol. 529, 2022. [CrossRef] [Google Scholar] [Publisher Link]

[17] Vincenzo Gattulli, and Marco Lepidi, "Nonlinear Interactions in the Planar Dynamics of Cable-Stayed Beam," *International Journal of Solids and Structures*, vol. 40, no. 18, pp. 4729-4748, 2003. [CrossRef] [Google Scholar] [Publisher Link]

[18] Vincenzo Gattulli et al., "One-to-Two Global-Local Interaction in a Cable-Stayed Beam Observed through Analytical, Finite Element and Experimental Models," *International Journal of Non-Linear Mechanics*, vol. 40, no. 4, pp. 571-588, 2005. [CrossRef] [Google Scholar] [Publisher Link]

[19] Peter Chang, and Xingzhuang Zhao, "Exact Solution of Vibrations of Beams with Arbitrary Translational Supports Using Shape Function Method," *Asian Journal of Civil Engineering*, vol. 21, no. 7, pp. 1269-1286, 2020. [CrossRef] [Google Scholar] [Publisher Link]

[20] Yaobing Zhao et al., "Effects of Temperature Variation on Vibration of a Cable-Stayed Beam," *International Journal of Structural Stability and Dynamics*, vol. 17, no. 10, 2017. [CrossRef] [Google Scholar] [Publisher Link]

[21] Christos Aloupis, Michael J. Chajes, and Harry W. Shenton III, "Damage Identification in Cable-Stayed Bridges Based on the Redistribution of Dead and Thermal Loads," *Engineering Structures*, vol. 284, 2023. [CrossRef] [Google Scholar] [Publisher Link]

[22] Vincenzo Gattulli, Massimiliano Morandini, and Achille Paolone, "A Parametric Analytical Model for Non-Linear Dynamics in Cable-Stayed Beam," *Earthquake Engineering Structural Dynamics*, vol. 31, no. 6, pp. 1281-1300, 2002. [CrossRef] [Google Scholar] [Publisher Link]

[23] Zhu Jun et al, "Nonlinear Dynamic Characteristics of Double-Cable Single-Beam Composite Structure," *Journal of Zhejiang University*, vol. 44, pp. 2326-2331, 2010. [CrossRef] [Publisher Link]

[24] V. Gattulli, and A. Paolone, "Planar Motion of a Cable-Supported Beam with Feedback Controlled Actions," *Journal of Intelligent Material Systems and Structures*, vol. 8, no. 9, pp. 767-774, 1997. [CrossRef] [Google Scholar] [Publisher Link]

[25] Chellapilla Kameswara Rao, "Frequency Analysis of Clamped-Clamped Uniform Beams with Intermediate Elastic Support," *Journal of Sound and Vibration*, vol. 133, no. 3, pp. 502-509, 1989. [CrossRef] [Google Scholar] [Publisher Link]